Suppression of the cardiac electric field artifact from the heart action evoked potential

J. J. Pérez[1] E. Guijarro[1] J. A. Barcia[2]

[1]Center for Research & Innovation on Bioengineering, Polytechnic University of Valencia, Valencia, Spain
[2]Department of Surgery, University of Valencia, Valencia, Spain

Abstract—*The study of heart action-related brain potentials is strongly disrupted by the presence of an inherent cardiac electric artifact. The hypothesis is presented that most of the electric current coupled to the cardiac field surrounds the skull and flows through the scalp tissue without crossing the cranial cavity. This pseudo two-dimensional conduction model contrasts with the volumetric conduction of the brain electrical activity, and this property is exploited to cancel the cardiac electric artifact. QRS loop vectorcardiographic projections on saggital planes were recorded in 11 healthy subjects in the head and neck areas. Comparative analysis of the projection eccentricities, estimated by the correlation coefficients of the paired data on each area, supported the hypothesis and allowed the handling of the cardiac electric field at the scalp as if enclosed in a two-dimensional wrapped space. This approach permitted the combination of different heart action-related brain potentials recorded at different electrode positions to cancel the cardiac electric artifact. The cancellation method, applied to the subjects' EEG data, yielded a slow cortical potential with a negligible cardiac electric residue and an amplitude of about 1.5–2 μV, with a maximum around 150 ms and a minimum at 400 ms post-R wave.*

Keywords—*Heartbeat evoked potential, Cardiac field artifact, Surface Laplacian, Skull electrical conductivity, Skull shielding effect*

Med. Biol. Eng. Comput., 2005, **43**, 572–581

1 Introduction

MULTIPLE NEURONAL interconnections between the vascular system and the brain are responsible for the influence of the heart cycle on the nervous system. Several authors have reported the enhancement of visual and auditory event-related potentials (ERPs) when the stimulus is synchronised with diastole but not with systole (SANDMAN *et al.*, 1984, 1992; CALLAWAY and LAYNE, 1964). Furthermore, it has been shown that the recurrent stimulation of the carotid sinus baroreceptors elicits a shift of a few microvolts on the cortical activity baseline, this effect being more pronounced in the frontal area (RAU *et al.*, 1993).

The existence of a specific response of the central nervous system to the heart action was first reported, simultaneously, by SCHANDRY *et al.* (1986) and JONES *et al.* (1986). They extracted this response from the EEG using the ERP approach by taking the R-wave of the ECG as a synchronous event to process the average. Since then, several research groups have studied this so-called heartbeat evoked potential (HEP), although, until now, a consensus about the morphology and topography of the HEP has not been reached. For example, RIORDAN *et al.* (1990) found that the maximum amplitude of the HEP was reached in a latency range of 120–160 ms post-R-wave; SCHANDRY *et al.* (1986) and JONES *et al.* (1988) found it between 200 and 300 ms; WEITKUNAT and SCHANDRY (1990) extended it within the range of 200–400 ms; MONTOYA *et al.* (1993) found it delayed to 350–550 ms; and DIRLICH *et al.* (1998) found a latency of the HEP of about 500 ms. Moreover, with regard to the topography of the HEP, most of these authors located the maximum amplitude of the HEP over frontal electrode positions, with the exceptions of RIORDAN *et al.* (1990) and LEOPOLD and SCHANDRY (2001), who observed it over the right anterior portion of the scalp, and DIRLICH *et al.* (1998), who located it over the parietal areas.

The HEP waveform seems to be extremely liable to become contaminated by several sources of artifact that are also synchronous with the heart cycle, mainly owing to the fact that HEP amplitude is scarcely of about 0.5–2 μV (DIRLICH *et al.*, 1998; SCHANDRY and MONTOYA, 1996). Formally, a signal extracted by simple averaging of several EEG sweeps time-locked with a stimulus can be considered as the sum of three different terms: first, a true response of the nervous system to the stimulus; secondly, a random residue of the EEG background activity and other asynchronous sources that have not been completely cancelled by the averaging process; and, finally, an electric potential caused by multiple non-neuronal sources, also synchronous with the stimulus (REGAN, 1989).

Correspondence should be addressed to Dr Juan J. Pérez; email: jjperez@eln.upv.es

Paper received 11 April 2005 and in final form 6 June 2005

MBEC online number: 20054039

These last kinds of artifact, which are time-locked with the stimulus, are of special relevance to the HEP recording. For example, the tremor caused on the electrodes by the arrival of the pressure blood wave at the underlying arteries can generate damped oscillations in the electrode potential (GEDDES and BAKER, 1989). For this reason, the use of elastic caps to fix the electrodes onto the scalp should be avoided (PEREZ *et al.*, 1999). Furthermore, these same artifacts have been observed in the HEP when the subjects lean their heads against a head support or use a neck roll to hold their head position (DIRLICH *et al.*, 1998).

On the other hand, the HEP is time-locked with the electrical activity of the heart. This electrical activity can also be recorded at the scalp surface and, although it is masked by the EEG in adult subjects, it can be observed in children (O'KELLY *et al.*, 1995) and even in brain-dead adults (JØRGENSEN, 1974). As a consequence, the HEP becomes strongly contaminated by the cardiac electric field (CEF). This inherent artifact has been observed by all the authors referenced here, and its topography on the scalp surface has been characterised by DIRLICH *et al.* (1997), who referred to it as the cardiac field artifact (CFA).

Several techniques have been proposed to remove the CFA from the HEP. The first attempt was made by SCHANDRY *et al.* (1986), who applied principal component analysis (PCA) to a set of HEP waveforms. They obtained five principal components, but CFA information seemed to be spread in more than one component. Later, SCHANDRY and WEITKUNAT (1990) proposed to cancel the CFA by subtracting from the EEG sweeps a cranial potential that was assumed to be caused solely by cardiac activity. For this purpose, they recorded the heart electrical activity at a location relatively free of EEG, in particular the tip of the nose, and simultaneously recorded the EEG at several standard electrode positions. Once the HEP at the scalp electrodes and the CFA at the tip of the nose were computed, they subtracted an adjusted ratio of the CFA from each HEP to minimise the variance of that difference in a selected time window around the R-wave of the ECG. This procedure has later been used by other authors to cancel the CFA (WEITKUNAT and SCHANDRY, 1990; KATKIN *et al.*, 1991; MONTOYA *et al.*, 1993), although, as some of them comment in their respective reports, some CFA residue still persists in their results.

On the other hand, DIRLICH *et al.* (1997), in an excellent work, approached the CFA problem from the vectorcardiographic point of view. They considered the HEP as the sum of a true evoked response, the generator of which would be located in the endocranial space, plus the projection on the scalp surface of a time-varying three-dimensional cardiac electric field. From this perspective, they tried to separate the true evoked response from the CFA by changing the relative position of both generators, brain and heart, by means of head turns. However, their results suggested that the scalp CFA distribution rotated only about 45% of the angle by which the head was turned in relation to the thorax. Finally, they proposed two strategies to study the HEP

(i) to limit the analysis to differential effects by comparing at least two HEP waveforms obtained under different experimental conditions, in which it should be assumed that the CFA did not change
(ii) to restrict the study to the refractory interval of the cardiac cycle, where the CFA should be considered nil.

This last strategy was used later by DIRLICH *et al.* (1998), but restricts the analysis to the range of 350–650 ms post-R-wave.

The present study focuses on the removal of the CFA from the HEP. For this purpose, first we will state and test a hypothesis about CEF distribution at the head area, according to which the markedly low electrical conductivity of the skull would cause most of the current lines generated by the CEF to flow through the scalp tissue without crossing the skull. This will confer on the scalp the property of being planar in the image space. In a second step, some CEF properties in the head area derived from the hypothesis will be used to remove the CFA from a set of HEP by means of their linear combination.

2 Materials and methods

2.1 *Hypothesis*

2.1.1 *Background and hypothesis statement*

The electrical characteristics and electric field distribution on the head have been studied in several biomedical areas. For example, the localisation of an epileptic focus to plan surgery may be estimated by modelling the epileptic focus as an electric dipole and inferring its localisation and orientation from EEG data recorded at multiple electrode positions (CUFFIN, 1998). Likewise, head impedance measured with both bipolar and tetrapolar electrode arrangements has been studied in transcranial impedance plethysmography, specifically known as rheoencephalography, to evaluate the cerebral blood flow (NYBOER, 1970; GEDDES and BAKER, 1989; PEREZ *et al.*, 2000).

In both issues, current distribution in the head caused by the current injection through two electrodes attached to the scalp has been studied. In these fields, of special relevance is the shielding effect of the skull caused by its low electrical conductivity in comparison with that of the scalp and brain. For example, RUSH and DRISCOLL (1968) showed experimentally that about 55% of the current injected by means of electrodes placed on the occipital and frontal areas flows through the scalp without crossing the endocranial space. Theoretically, the maximum amount of current flowing through the skull can be obtained by reducing the electrode size and placing the electrodes at opposite sides of the head (PEREZ *et al.*, 2000). Moreover, even when the electrode size becomes nil, more than 33% of the injected current does not cross the skull (MALMIVUO and PLONSEY, 1995).

On the other hand, the CEF can be described by an electric dipole at points relatively far from the heart (MALMIVUO and PLONSEY, 1995). Under this perspective, the CFA would be caused by the current lines coupled to the CEF that emerge from the heart, flow through the neck, reach the head and return by the same path to the electric dipole. Therefore the CEF in the head area can be seen as a far field in contrast to the one created by the direct current injection using electrodes attached to the scalp surface. Hence, it seems reasonable to expect that the current lines coupled to the CEF will flow predominantly through the scalp tissue without crossing the skull, in preference to a path in which current lines cross the skull, enter the endocranial space and emerge again from the skull to reach the scalp.

Based on this reasoning, the hypothesis stated here is that most of the flow lines of the CEF go around the skull through the scalp tissue, the current lines that cross the cranium being minimal.

2.1.2 *Hypothesis test*

The working hypothesis is based on the assumption that the low conductivity of the skull produces an electrical shielding effect on the brain, insulating it from the electric field generated by the heart. As a consequence, the flow lines of the CEF should reach the vertex of the head through the scalp tissue, without crossing the skull.

To understand the properties of the CEF in the scalp area derived from the hypothesis and how these properties can be

used to test the hypothesis and to remove the CFA from the raw HEP, it may be helpful to develop several successive approximations. First, let us consider an isotropic, homogeneous and infinite two-dimensional surface where an electric uniform field $\boldsymbol{E}$ created by a distant dipole exists (Fig. 1*a*). If points A, B, C and D are equidistant from the *X*-*Y*-axis origin O and are aligned as shown in Fig. 1*a*, $U_{OA} + U_{OB} = 0$ and $U_{OC} + U_{OD} = 0$, where U_{MN} is the electric potential of point N with respect to that of point M. It should be noticed that these equations are independent of the direction of vector $\boldsymbol{E}$ and are valid even for time-varying vector parameters, as occurs in the CEF. In this Figure, the grid can be interpreted as the isopotential lines created by a distant source at two selected dipole orientations.

Now, let us suppose that the planar surface of the previous reasoning is not a two-dimensional area, but has a small and slightly variable thickness that keeps geometric symmetry with respect to the *Y*-axis. In this case, the electric field $\boldsymbol{E}$ will not be uniform, the grid will be distorted, and the concept of collinear points will be not evident. In spite of this, points A, B and O can be considered to be arranged on the same line because of the symmetry of the whole set with respect to the *Y*-axis. Nevertheless, it must be taken into account that the distance O–A cannot be regarded as identical to O–B in the electrical sense, because of the absence of symmetry with respect to the *X*-axis. Therefore, although the absolute values of U_{OA} and U_{OB} are not identical, they are linearly dependent. This, then, can be written as

$$U_{OA} + \lambda_Y U_{OB} = 0 \tag{1}$$

where the cancellation coefficient λ_Y is constant if the spatial second derivatives of the scalar field U are negligible. Note that, again, (1) is independent of the direction and magnitude of the electric field. This means that, although vector $\boldsymbol{E}$ rotated as does the CEF, the scalar composition expressed in (1) of the electric potentials U_{OA} and U_{OB} remains nil at every time.

As described above, the electric field gradient has the result that the spatial and electrical distances do not match. Intuitively, it can be seen as if the orthogonal grid of Fig. 1*a* had been transformed to that of Fig. 1*b* by the electric field gradient. In this new grid, points C, D and O are not collinear, and thus, despite the spatial symmetry of the arrangement with respect to the *Y*-axis, the plain sum of the electric potentials U_{OC} and U_{OD} will not be nil as in the case of the uniform electric field. To solve this, let us now consider that we distort the surface of Fig. 1*b* depending on the electric field gradient, as if the whole were made with an elastic material, until we again obtain an orthogonal grid (Fig. 1*c*). This will allow us to go on with the reasoning as if the electric field were uniform. As a result of the distortion, point O is now displaced towards B, causing the plain sum of the potential differences U_{OC} and U_{OD} to be not nil. Furthermore, according to this approach, the plain sum of U_{OC} and U_{OD} can be expressed as a function of U_{OA} or U_{OB} or, in other words, can be cancelled by any of them even for time-varying electric fields. This assertion can be written as

$$(U_{OC} + U_{OD}) + \lambda_X U_{OB} = 0 \tag{2}$$

where the cancellation coefficient λ_X is constant.

Finally, let us consider that the described planar surface is wrapped to cover the cranium and to become the scalp tissue. The anatomical symmetry with respect to the midsagittal plane (*Y*-axis direction) is approximately true, although it lacks in the coronal plane (*X*-axis direction). The heart is sufficiently distant from the scalp to consider the CEF as a far field at the head area. Obviously, CEF variations along the scalp area due to its curvature follow complex rules, not covered by the approach; however, the anatomical symmetry with respect to the midsagittal plane is present.

A similar line of reasoning can also be followed by addressing the scalp model from the point of view of lead vector concepts. In this sense, the electrical activity of the heart can only be described in the three-dimensional space, as the equivalent cardiac dipole rotates spatially. In general, the image space of an arbitrary volume of tissue will also be a three-dimensional space, because current created by the cardiac dipole can flow in any direction. However, according to the hypothesis, the flow lines caused by the heart activity are enclosed in a two-dimensional wrapped space, i.e. the scalp tissue, and therefore the image space of the scalp would be a plane similar to that shown in Fig. 1*c*.

In this study, the model described above is applied to the scalp tissue to test the hypothesis and to remove the CFA from the HEP. According to the model, and if the hypothesis were true, i.e. the flow lines of the CEF reached the vertex of the head through the scalp tissue without crossing the cranium, given the symmetry of the head with respect to the midsagittal plane, a phase diagram composed of two CFAs collected between electrodes placed on the scalp surface at the midsagittal plane should produce a straight line, showing that one CFA is a linear combination of the other. However, if the hypothesis were false, i.e. the flow lines of the CEF crossed the head as if the head were homogeneous and isotropic, a phase diagram registered on the scalp surface at the midsagittal plane should not be necessarily a straight line and, moreover, it should not be specially different from an other phase diagram recorded, for instance, on the neck area.

The design of an experiment to test the hypothesis using the aforementioned theoretical concepts requires the recording of a

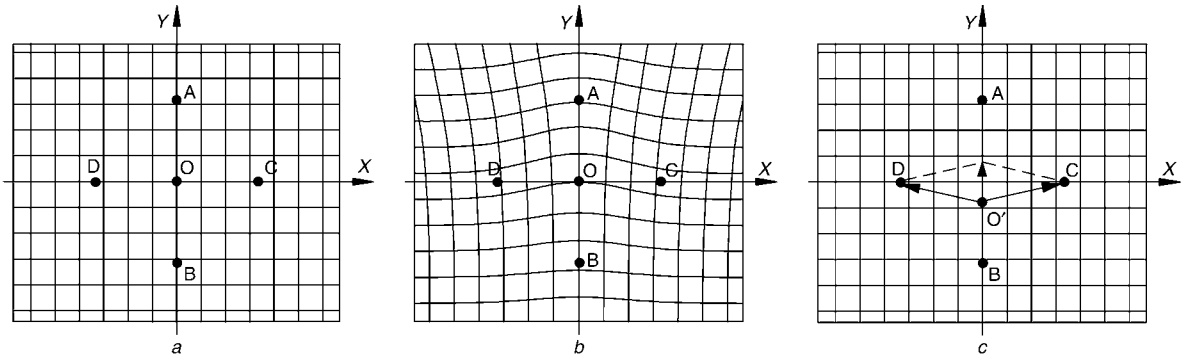

Fig. 1 *Planar surface models of the scalp. (a) Two-dimensional surface with a regular grid. (b) Thin sheet of slightly variable thickness with symmetry with respect to the Y-axis, in which the regular grid is distorted by the electric field gradient. (c) Same model as (b), but with spatial grid regularised*

pure CFA at scalp localisations. However, the CFA at the scalp electrodes will always be mixed with the EEG activity and, in fact, although EEG background amplitude could be reduced by averaging cardiac activity time-locked EEG sweeps, averaged CFA will be inherently mixed with the HEP. In this paper, the CFA study is restricted to the QRS time interval of the raw HEP.

Preliminary results showed that the CFA had a mean intra-individual amplitude of 7 μV in that interval, whereas HEP amplitude did not exceed 2 μV during the whole cardiac cycle. Similar approaches have been used by other authors to analyse CFA and HEP waveforms separately (MONTOYA *et al.*, 1993; DIRLICH *et al.*, 1997).

2.1.3 *CFA cancellation*

Let us suppose in this Section that the hypothesis is true. Then, the CFA can be removed from the HEP by exploitation of their differences on the conduction pathway as follows. On the one hand, current lines that produce the CFA waveform are enclosed, according to the hypothesis, in a wrapped two-dimensional surface (scalp) and should satisfy (1) and (2). On the other hand, the HEP recorded at the scalp surface requires a volumetric pathway, as its generator is located inside the head. Owing to the head symmetry with respect to the midsagittal plane, the CFA waveforms of the raw HEPs recorded between any pair of electrodes placed on that plane should be morphologically constant. This means that the CFA can be cancelled by application of (1) to two raw HEPs recorded at the midsagittal plane. Moreover, the plain sum of two CFA waveforms recorded from pairs of electrodes placed on the coronal plane and symmetrically to the midsagittal plane will not cancel the CFA because of the lack of head symmetry with respect to the coronal plane. However, the result of this sum will produce a CFA waveform morphologically identical to that obtained from any pair of electrodes placed on the midsagittal plane and can be cancelled by means of (2).

2.2 *Subjects and electrodes*

Eleven healthy volunteers, nine male and two female, aged between 24 and 45 years (mean 34.7 years) participated in the experiment. The subjects had no history of cardiac or neurological disorders and, prior to the experiment, were formally informed about its purpose. The relevance of the cardiac cycle in the experiment was not mentioned to avoid subjects paying special attention to their own heartbeat (SCHANDRY and MONTOYA, 1996).

The experiment took place in a sound-attenuated, air-conditioned room designed to achieve the maximum relaxation of the subjects. They were seated in a comfortable desk chair, slightly tilted, in such a way that their heads did not rest on the chair back. The subjects were asked to keep their heads balanced to reduce electromyogram and movement artifacts. All the technical instrumentation and accessories were behind the subjects, and a television set was placed 1.5 m in front of them, on which a soothing documentary was played during the preparatory and pre-recording stages.

After the scalp sites had been rubbed with sandpaper and cleaned with alcohol, 1 cm diameter Ag/AgCl electrodes* were placed at Fpz, Cz, Oz, C5 and C6, according to the international 10–20 system (JASPER, 1957) and attached with electrode cream (Fig. 2). Electrode leads were fixed to the skin over the cranium structure with sticking plaster at least two points to reduce the influence of the subject's movement relative to the amplifiers caused by the heartbeat (PEREZ *et al.*, 1999).

As will be described later, the electrodes placed at Fpz, Cz and Oz were used to obtain a phase diagram on the midsagittal plane at the head area. To compare this CEF projection with the other one recorded from an area proximal to (but not in) the head, three adhesive electrodes were placed on the left side of the neck in an equivalent geometrical arrangement (Fig. 2). The electrode equivalent to Cz, labelled NR, was placed 1 cm below the left mastoid. The other two, equivalent to Fpz and Oz and labelled NA and NP, respectively, were placed 3 cm apart from NR. Special care was taken to ensure that the line segments NA–NR and Fpz–Cz on the one hand, and NP-NR and Oz–Cz on the other, were approximately parallel among them.

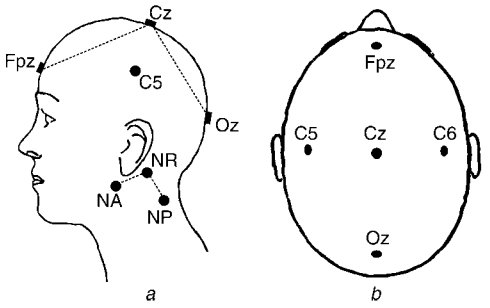

Fig. 2 *(a) Lateral and (b) top views of head electrode positions used in the experiment*

To determine the onset and end of the QRS loop of the CEF, the ECG was recorded in three different directions. ECG stainless electrodes were placed on both arms and on the left leg, and, additionally, two adhesive electrodes were attached: one 1 cm below the superior border of the sternum (SE) and the other in the same horizontal plane over the vertebral column (VE).

2.3 *Data recording*

Once the electrodes had been placed and connected to the amplifiers, the television set and lights were switched off. The subjects were asked to close their eyes, and to relax and be asleep as deeply as possible to minimise alpha waves on the EEG. Before the start the recording, a rest time of 5 min was given to allow for subject adaptation (pre-recording stage).

The EEG was recorded at scalp electrodes referenced to Cz, and the ECG at NA and NP was referenced to NR. Additionally, ECG leads I and III and the signal derived from SE with respect to VE were recorded. All signals were amplified using Biopac amplifiers† with a bandwidth of 0.1–35 Hz and stored in a computer making use of a 12-bit acquisition card for further processing. To achieve high resolution in the QRS loops, channels were acquired at 5000 sample s^{-1}. Amplification gains were adjusted during the pre-recording stage to ensure that no channel would become saturated during the recording stage. Once the subject was relaxed, and the amplifier gains were adjusted, channels were acquired for 900 s.

2.4 *Data processing*

All signal analysis in this study was performed using the average of the data sweeps time-locked with the R-wave of lead I and extended from 100 ms prior to the R-wave to 700 ms after it.

To determine the synchronous references so that the averages could be computed, a preliminary set of fiducial points was obtained by detecting the R-wave of lead I with the algorithm proposed by PAN and TOMPKINS (1985) and slightly modified by HAMILTON and TOMPKINS (1986). Finer

*Astro-Med, Inc., RI, USA

†Biopac Systems, Inc., CA, USA

selection and adjustment of the synchronism were achieved by means of the following procedure: averaging of lead I sweeps time-locked with the preliminary set of fiducial points in an arbitrary time window of 120 ms length, starting 12 ms prior to them; then, using this average as a template, correction of the jitter of each lead I sweep relative to the template by its cross-correlation function; and, finally, rejection of the sweeps with a maximum in that function lower than 0.9. The selected time window was chosen to cover the QRS complex and seems apparently off-centre because the fiducial points obtained with this algorithm were actually closer to the Q-wave than to the R-wave.

The fiducial points obtained in this way for each subject were used as synchronous events to obtain the projection of the QRS loop of the CEF on each recording channel (leads I and III, SE–VE, NA–NR, NP–NR, and Fpz, Oz, C5 and C6 referenced to Cz). To this end, ECG channels (leads I, III and SE–VE) were averaged and, for each subject, the narrowest temporal window in which the QRS loop of the CEF could be enclosed (QRS loop time window) was manually established from the three ECG lead averages and their derivatives. Then, the projections of the QRS loop at the neck and scalp localisations were obtained by averaging the recordings at these areas (Fpz, Oz, C5, C6, NA and NP sites with respect to their respective references) within the individual selected time window.

To test the hypothesis, the projection of the QRS loop on the midsagittal plane at the scalp area from the composition of the QRS complex at Fpz and Oz was compared with that obtained at the neck area from the QRS complex at NA and NP.

The following procedure was used to derive two CFA-free HEP waveforms. First, the original EEG data recorded at Fpz, Oz, C5 and C6 and lead I were decimated to an equivalent sample frequency of 500 samples s^{-1}; secondly, the R-waves of lead I were detected, and the fiducial points were corrected, as described above; finally, the EEG sweeps at each electrode extending from 100 ms prior to the R-wave to 700 ms after it were averaged. This procedure generates four raw HEPs at the scalp recording electrodes.

The CFA of each HEP waveform was cancelled using the approach described. Under our hypothesis, the CFA contained in the HEP at Fpz was assumed to be proportional to that at Oz. Therefore the cancellation coefficient in the midsagittal plane λ_S for each subject was estimated by the slope of the regression line of the previously obtained projections of the QRS loop at Oz and Fpz, using the high sample rate registers. Following a similar procedure, the cancellation coefficient in the coronal plane λ_C was assessed for each subject by the slope of the regression line of the plain sum of the QRS loop at C5 and C6, with respect to that obtained at Oz. It should be noted that the assessment of the cancellation coefficients λ_S and λ_C was restricted to the QRS loop time-window, because the relative amplitude of the CFA in the HEP is higher.

Once the cancellation coefficients for each subject were calculated, a CFA-free HEP in the midsagittal plane was obtained by the weighted sum of the raw HEP recorded at Fpz and Oz. This approach can be expressed as

$$\Phi_S = Fpz + \lambda_S Oz \tag{3}$$

where Φ_S is a sagittal CFA-free HEP waveform, Fpz and Oz are the raw HEPs at such electrodes, and λ_S is the associated cancellation coefficient.

In the same manner, a second CFA-free HEP waveform Φ_C was obtained from each subject by combination of the sum of the raw HEPs at C5 and C6 with their respective HEP at Oz. It can be expressed as

$$\Phi_C = (C5 + C6) + \lambda_C Oz \tag{4}$$

where Φ_C is the new CFA-free HEP waveform, $C5$ and $C6$ are the raw HEP at such electrodes, and λ_C is its respective cancellation coefficient.

3 Results

3.1 *CEF projection on the sagittal plane at neck and head areas*

After a close inspection of the averaged potentials obtained in each subject (four raw HEP waveforms and the ECG at NP and NR leads), those recorded from subjects V04 and V09 were discarded because of technical problems not detected during the recording stage.

Figure 3*a* plots the QRS complexes recorded at NP against the one at NA for each subject, normalised to unit variance. Each curve can be considered as a rough projection on the sagittal plane of the subject's CEF at the left side of the neck. These same projections, but recorded at Oz and Fpz, are shown in Fig. 3*b*.

Inter-individual variability of the QRS loop at the neck is significant: some subjects show a nearly circular QRS loop, whereas others present a highly eccentric loop. However, the

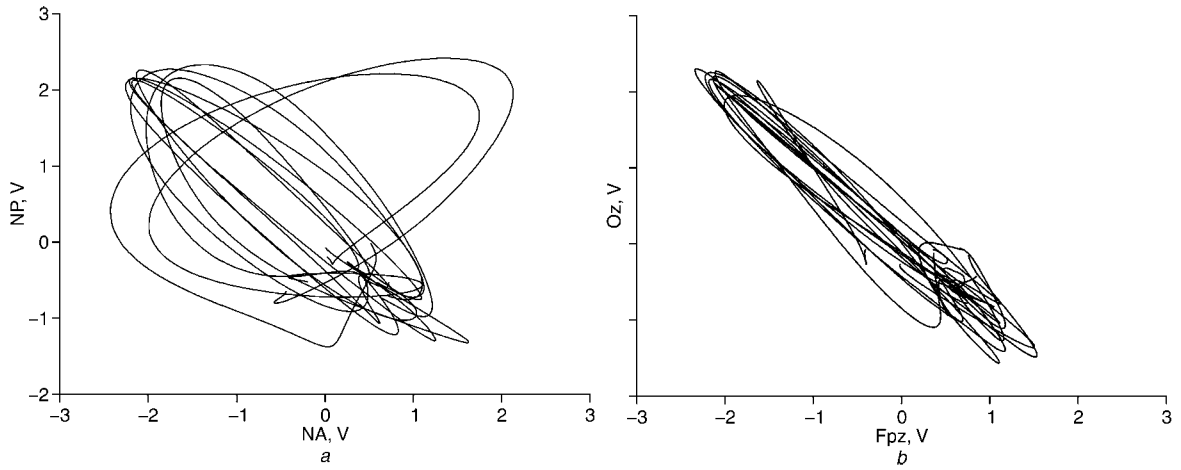

Fig. 3 *Plots of the paired data recorded within the QRS time window at (a) neck (NP–NA) and (b) head (Oz–Fpz) for each subject and normalised to unit variance*

Table 1 Correlation coefficients between each pair of QRS complexes recorded at neck (NP–NA) and at head (Oz–Fpz) for each volunteer. Mean and 95% confidence interval assessed using Fisher transform

Subject	ρ (NP–NA)	ρ (Oz–Fpz)
V01	−0.90	−0.91
V02	−0.91	−0.99
V03	0.17	−0.92
V05	−0.98	−0.97
V06	0.42	−0.95
V07	−0.96	−1.00
V08	−0.95	−0.96
V10	−0.72	−0.99
V11	−0.80	−0.97
Mean	−0.83	−0.97
CI ($\alpha = 0.05$)	−0.99–−0.60	−0.99–−0.88

QRS loop recorded at the head electrodes shows an intense eccentricity for any subject.

The correlation coefficients between each pair of QRS complexes recorded at the neck (NP and NA referenced to NR) and at the head (Oz and Fpz referenced to Cz) for each volunteer are given in Table 1. As can be inferred from Fig. 3, the correlation coefficients between the pairs of QRS complexes at the neck area are notably more scattered than those at the head. Statistically significant differences have been found between paired correlation coefficients using the Fisher transform (t-test, $n = 9$, $p < 0.01$). Moreover, it can also be observed that, for any subject, the absolute value of the correlation coefficient between Oz and Fpz is always higher than that obtained between NP and NA, with the exception of subject V05, in which both are near the unity.

3.2 *Raw HEP waveforms*

After processing of the individual raw HEP waveforms, the data derived from subject V09 were discarded because of technical problems. Moreover, the HEP waveforms obtained at electrodes C5 and C6 of subjects V06 and V08 revealed a strong damped oscillation, probably caused by the tremor of the temporal superficial artery. These data were not used to compute the grand averages (GAs).

Figure 4 shows the GA waveforms derived from 10 410 EEG sweeps recorded on the midsagittal plane at Fpz and Oz. Both raw HEP waveforms show strong interference caused by the CEF, the QRS complex and the T-wave being clearly identifiable. The broken-line band, framing the evoked response, delimits the 95% confidence interval of the mean at every sample time and emphasises the outline of the waveform. Within the interval from 350 ms to 650 ms post-R-wave, where the CFA amplitude can be considered negligible (DIRLICH *et al.*, 1998), the HEP at Fpz shows non-iso-electric activity.

The raw GA waveforms recorded on the coronal plane at C5 and C6 and their respective band of confidence interval are shown in Fig. 5, composed of 8348 sweeps. As before, there is an intense QRS artifact in both recordings, although, in contrast to the midsagittal registers, QRS loop projections at C5 and C6 are clearly not in phase. It can also be observed that both HEP waveforms rise during the refractory period of the cardiac cycle.

3.3 *CFA cancellation*

A close inspection of the QRS artifacts in the raw GA waveforms at Fpz and Oz (Fig. 4) shows that the R-wave occurs simultaneously, or, in other words, the QRS complexes appear inverted and in phase.

On the other hand, this property is not present in the GA waveforms recorded on the coronal plane at C5 and C6 (Fig. 5). Moreover, although the R-wave occurs simultaneously in both waveforms, the GA obtained at C5 (Fig. 5*a*) shows a biphasic QRS complex, whereas that obtained at C6 (Fig. 5*b*) is monophasic.

However, the plain sum of the raw HEP recorded at C5 and C6 provides a similar QRS projection to that projected on the midsagittal plane (Fig. 6). Fig. 6 shows the sum of the HEP at C5 and C6 (Fig. 6*a*) and the HEP at Oz derived from the same subject set (Fig. 6*b*).

After the calculation of the cancellation coefficients λ_S and λ_C for each subject and the composition of their records as described in Section 2 using (3) and (4), the GA waveforms of the CFA-free HEP were obtained in both planes, as shown in Fig. 7. This Figure shows the GA of Φ_S and Φ_C, framed by the 95% confidence interval of the mean at every sample time. A minor residue of the QRS complex seems to persist despite the cancellation method, although its amplitude is minimal in comparison with the amplitude of the potential. Both curves show similar outlines and seem to be composed of two components: a major slow wave and an overlapped fast-wave. The slow-wave frequency seems to match the heart rate, and its amplitude is about 1.5–2 μV and shows an ascendant phase to reach the maximum value at about 150 ms post-R-wave; a subsequent descending phase to reach

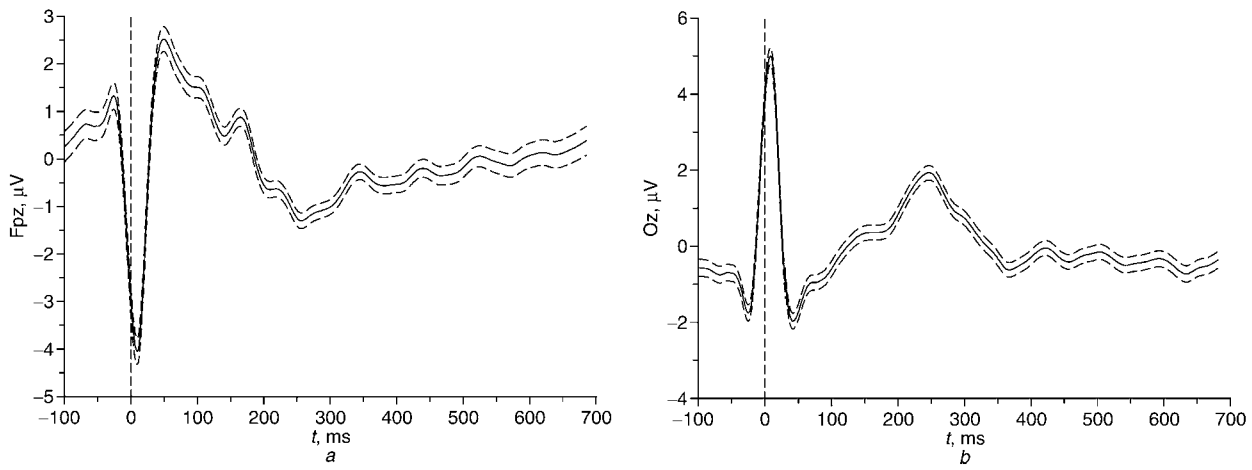

Fig. 4 *Grand average of the HEP at (a) Fpz and (b) Oz. (—) HEP; upper and lower broken lines, 95% confidence interval of the mean at every sample time. n = 10 410; data from V09 were discarded*

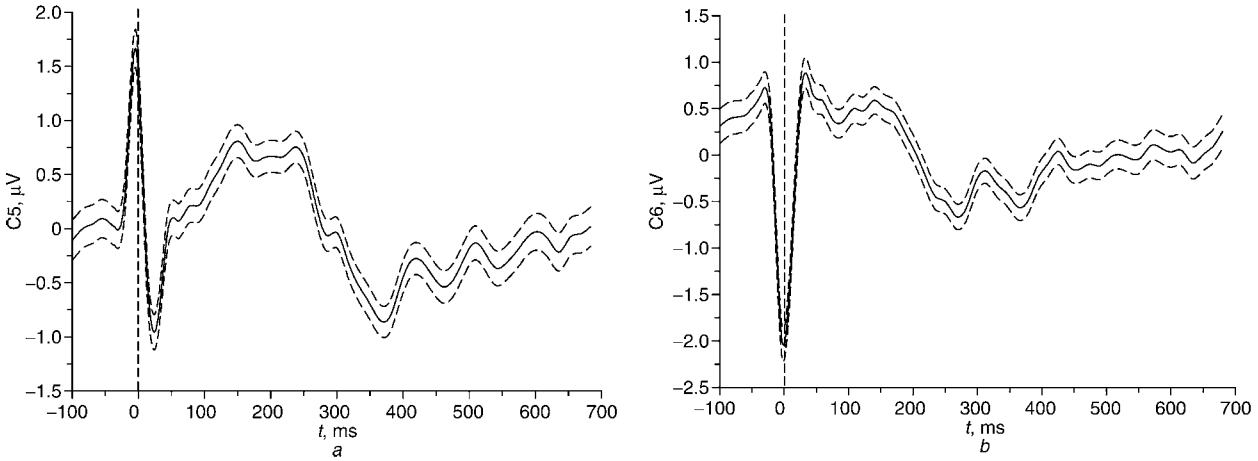

Fig. 5 *Grand average of the HEP at (a) C5 and (b) C6. (—) HEP; upper and lower broken lines: 95% confidence interval of the mean at every sample time. n = 8348; data from V06, V08 and V09 were discarded*

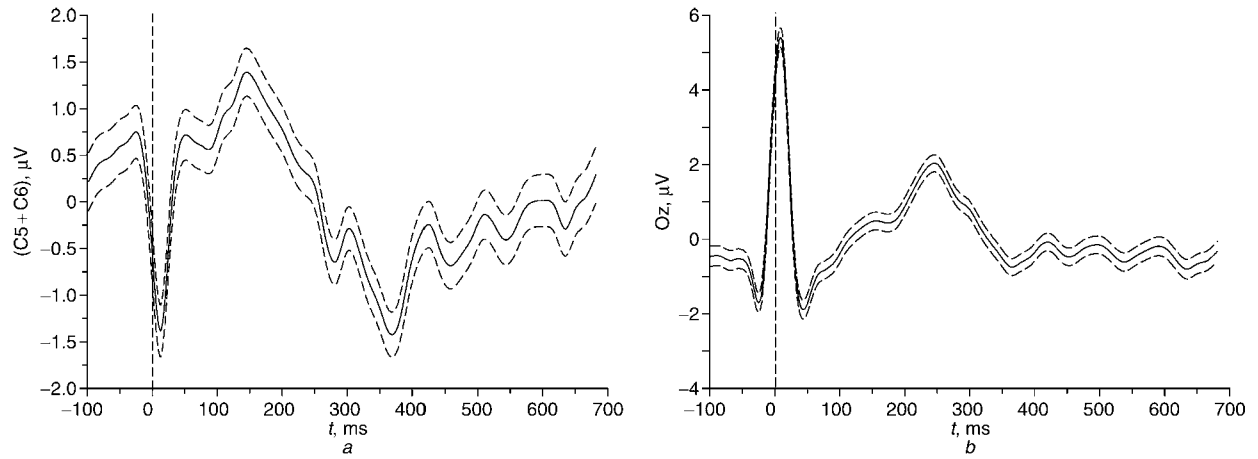

Fig. 6 *(a) Grand average of sum of HEP at C5 and C6; (b) grand average of the HEP at Oz obtained from the same set of subjects (—) HEP; upper and lower broken lines: 95% confidence interval of the mean at every sample time n = 8348; data from V06, V08 and V09 were discarded*

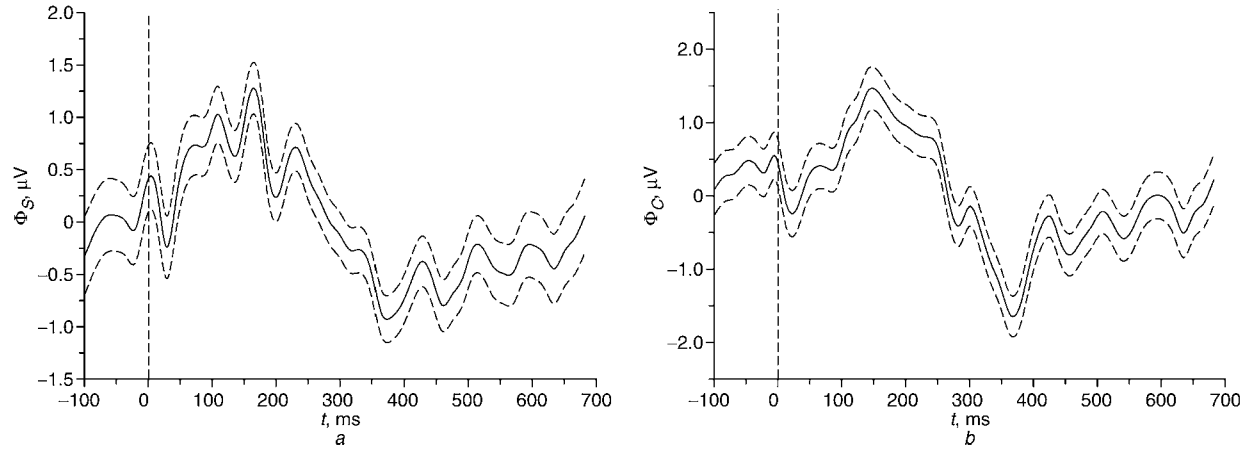

Fig. 7 *Grand average of the HEP waveforms obtained after CFA cancellation. (a) Φ_S potential obtained by the weighted sum of the HEP at Fpz and Oz; n = 10410; data from V09 were discarded. (b) Φ_C potential obtained by the weighted sum of the HEP at C5, C6 and Oz n = 8,348; data from V06, V08 and V09 were discarded. (—) Φ_S and Φ_C; upper and lower broken lines: 95% confidence interval of the mean at every sample time*

the minimum amplitude at about 400 ms; and a final ascending phase to recover its original value. The fast-wave is an irregular component, with an estimated frequency of about 11 Hz, that extends along the recorded interval.

4 Discussion

Since SCHANDRY *et al.* (1986) and JONES *et al.* (1986) reported the existence of an evoked response time-locked to the heartbeat until now, the study of the HEP has been

restricted to differential analysis or to the refractory interval of the cardiac cycle, because of the presence of strong electrical interference caused by the CEF.

Although the QRS complex is clearly visible in the HEP, and it does not avoid outlining the evoked response, the T-wave occurs within the range of the likely latency of the HEP, and both can be easily misinterpreted. For this reason, most CFA analysis focuses on the QRS complex, where most of the HEP variance can be explained by the heart activity (DIRLICH *et al.* 1997).

However, it must be kept in mind that the CEF is a vector defined in a three-dimensional space; thus the CFA cannot be removed using exclusively the information derived from a single ECG lead. Moreover, although it was assumed that each loop of the CEF was planar, QRS and T loops may not be coplanar and even may define an angle up to 30° in some subjects (FISCH, 1997). Hence, knowledge about the rules by which the QRS loop is projected onto the scalp only gives information about the projection of a two-dimensional subspace, and additional data are necessary for us to know how the T loop is projected onto the scalp.

On the other hand, DIRLICH *et al.* (1997) showed that the scalp CFA distribution rotated only by about 45% of the angle by which the head was turned in relation to the thorax. As they pointed out in their report, this result shows the geometrical complexity of the propagation rules of the cardiac electric field with regard to the scalp. In fact, the electrical characteristics of the neck tissues are notably anisotropic. For instance, most of the muscular fibres of the neck are aligned in the body axis direction, and the electrical conductivity of the muscular fibres in the longitudinal direction is 13 times greater than that in the transverse direction (BARBER, 1995). Likewise, blood conductivity is relatively high, and the main vessels within the neck are also aligned with the body axis. Therefore, when the head turns in relation to the thorax, the preferential direction of the current flow also twists, causing the observed decrement in the rotation angle of the CFA.

In this work, we have stated the hypothesis that most of the CEF flow lines go around the skull through the scalp tissue, the current lines that cross the cranium being minimal. If the electrical characteristics of the neck and head were homogenous and isotropic, the QRS loop projection on the sagittal plane at the head and at the neck would be slightly, but not extremely, different. The fact, for example, that in subject V07 the correlation coefficient between the pair of QRS complexes at the neck was -0.96 and at the head was -1.00 (Table 1) is not relevant. However, an isotropic and homogeneous head model does not explain that, in subject V03, the correlation coefficient of the pair of QRS complexes was 0.17 at the neck and -0.92 at the head.

Specifically, despite the high inter-individual variability of the correlation coefficients at the neck, the coefficients obtained at the head lie within the range of -0.91 to -1.00, where it must be taken into account that the QRS complexes recorded at the head are disturbed by HEP and residues of EEG background activity. This result provides strong evidence to support our hypothesis. Although the hypothesis test has been made from the data set corresponding to the QRS complexes, it must be noted that its consequences involve the whole cardiac cycle, including the T-wave.

According to our hypothesis, and owing to the head symmetry in relation to the midsagittal plane, the CFA waveforms included in the HEP at Fpz and Oz reference to Cz should be morphologically identical, as has been noticed in the QRS time window. However, although the Fpz and Oz electrode positions are equidistant from Cz, the plain sum of the HEP at Fpz and Oz fails to cancel the CFA because of the lack of head symmetry with respect to the coronal plane. The λ_S required to cancel the CFA have been assessed by means of the slope of the linear regression of the HEP paired data at Oz and Fpz within the QRS time window, this coefficient being characteristic of each subject.

On the other hand, and as a consequence of the lack of head symmetry in the coronal plane, the CFA on the HEP at C5 and C6 shows the QRS complexes clearly out of phase (Fig. 5). However, such positions are symmetrical with respect to the midsagittal plane, and the plain sum of both of their HEPs provides a CFA whose QRS complexes are in phase with those obtained at the sagittal HEP (Fig. 6). This result provides a new proof that confirms our hypothesis. To cancel the CFA from the sum of the central HEP waveforms, we have chosen the HEP at Oz, as it seems to involve minor activity within the time window of the refractory heart cycle.

The result of both cancellation processes has been shown in Fig. 7. It must be observed that potentials Φ_S and Φ_C present a small oscillation around the co-ordinate origin. This could be interpreted as a residue of the QRS complex; however, its appearance and amplitude are similar to the fast component visible along all the potential. Nevertheless, supposing that this oscillation were a trace of the QRS complex, the broad peak reached at 150–200 ms post-R-wave cannot be explained by the T-wave, taking into account that the attenuation of the CFA should be uniform throughout the cardiac cycle, as can be inferred from our hypothesis. This consideration allows us to draw the morphology of CFA-free HEP waveforms as the sum of two components: a slow wave, whose period matches the cardiac interval length and of about 2 μV amplitude, and of a fast irregulaR-wave of about 11 Hz, with an amplitude in the order of 0.5 μV. This fast component can also be observed in the reports of some other authors (see, for example, MONTOYA *et al.*, 1993) and it could be due either to residues of EEG alpha waves that have not been completely cancelled by the averaging, or to synchronous electromechanical artifacts caused by the tremor of the electrode leads.

The slow waves at Φ_S and Φ_C have a similar morphology, despite the fact that both of them were obtained by the combination of HEP waveforms at different electrodes, with the exception of the minor contribution to Φ_C of the HEP at Oz. In conclusion, the HEP waveform can be described as a slow potential of about 2 μV amplitude that shows a peak at 150–200 ms post-R-wave and a minimum at 400 ms. This is the first time, as far as we know, that an HEP waveform has been described for the entire cardiac period with negligible cardiac electric interference.

A final consideration involves the physical meaning of Φ_S and Φ_C potentials. Both are obtained by the combination of at least two HEP waveforms recorded at distanced electrodes. For example, the Φ_S potential is the result of the weighted sum of the HEP at Fpz and Oz, adjusted to ensure that the contribution to the Φ_S potential of the currents coupled to the CEF be nil, or, in other words and according to our hypothesis, that the Φ_S sensitivity to currents tangential to the head surface be nil.

A similar reasoning can be applied to the Φ_C potential with the particularity that it is composed of three HEP records. This same property defines the surface Laplacian, which can be estimated by the sum of the potentials recorded from at least four electrodes uniformly arranged and equidistant to a reference electrode (HE, 1997). A more accurate assessment of the surface Laplacian considers the curvature of the surface defined by the electrodes (OOSTENDORP and OOSTEROM, 1996) and the scalp thickness (BABILONI *et al.*, 1997). Its magnitude is proportional to the spatial derivative, on the normal direction to the electrode surface, of the current density component in such a direction (HE, 1997).

In practice, the distance between electrodes used to measure the surface Laplacian is significantly shorter than the one used in this work. However, the fact that the physical basis of both the Φ_S and Φ_C potentials and the surface Laplacian were essentially identical suggests that the Φ_S and Φ_C potentials are likely to reflect the current density emerging from the brain to the scalp surface with a magnitude proportional to its spatial derivative on the normal direction.

5 Conclusions

The study of heart action-related brain potentials is restricted because the evoked response is strongly contaminated by cardiac electrical activity, which is, by definition, synchronous with the brain response. The experimental results support the hypothesis that most of the current flow lines of the CEF go around the skull through the scalp tissue, the current lines that cross the cranium being minimal. This feature of the CEF allowed us to cancel the CFA by the appropriate combination of several HEP waveforms. Finally, two CFA-free evoked responses were obtained, showing a waveform that can be described as a slow potential of about 2 μV amplitude, with a peak at 150–200 ms post-R-wave and a minimum at 400 ms

Acknowledgments—The authors thank Dra Asuncion Moreno and Dra Claudia Zarate for their valuable scientific comments about the measurement methodology, and the ACLE service of the UPV for the English revision.

This research was partially supported by grants GV00-105-12 and UPV-19990551, and by the 'Programa de Incentivo a la Investigación' of the Polytechnic University of Valencia.

References

BABILONI, F., BABILONI, C., CARDUCCI, F., DEL GAUDIO, M., ONORATI, P., and URBANO, A. (1997): 'A high resolution EEG method based on the correction of the surface Laplacian estimate for the subject's variable scalp thickness', *Electroencephalogr. Clin. Neurophysiol.*, **103**, pp. 486–492

BARBER, D. C. (1995): 'Electrical impedance tomography', in BRONZINO, J. D. (Ed.): 'The biomedical engineering handbook' (CRC Press, Boca Raton, 1995), pp. 1151–1164

CALLAWAY, E. and LAYNE, R. (1964): 'Interaction between the visual evoked response and two spontaneous biological rhythms: the EEG alpha cycle and the cardiac arousal cycle', *Ann. New York Acad. Sci.*, **112**, pp. 421–431

CUFFIN, B. N. (1998): 'EEG dipole source localization', *IEEE Eng. Med. Biol. Mag.*, **17**, pp. 118–122

DIRLICH, G., VOGL, L., PLASCHKE, M., and STRIAN, F. (1997): 'Cardiac field effects on the EEG', *Electroencephalogr. Clin. Neurophysiol.*, **102**, pp. 307–315

DIRLICH, G., DIETL, T., VOGL, L., and STRIAN, F. (1998): 'Topography and morphology of heart action-related EEG potentials', *Electroencephalogr. Clin. Neurophysiol.*, **108**, pp. 299–305

FISCH, C. (1997): 'Electrocardiography', in BRAUNWALD, E. (Ed.): 'Heart disease: a textbook of cardiovascular medicine' (Saunders Company, New York, 1997), pp. 108–152

GEDDES, L. A. and BAKER, L. E. (1989): 'Principles of applied biomedical instrumentation' (Wiley, New York, 1989)

HAMILTON, P. S. and TOMPKINS, W. J. (1986): 'Quantitative investigation of QRS detection rules using the MIT/BIH arrhythmia database', *IEEE Trans. Biomed. Eng.*, **33**, pp. 1157–1165

HE, B. (1997): 'Principles and applications of the Laplacian electrocardiogram', *IEEE Eng. Med. Biol. Mag.*, **16**, pp. 133–138

JASPER, H. H. (1957): 'The ten twenty electrode system of the international federation', *Electroencephalogr. Clin. Neurophysiol.*, **28**, pp. 173–179

JONES, G. E., LEONBERG, T. F., ROUSE, C. H., and SCOTT, D. M. (1986): 'Preliminary data exploring the presence of an evoked potential associated with cardiac visceral activity', *Psychophysiology*, **23**, p. 445

JONES, G. E., ROUSE, C. H., and JONES, K. R. (1988): 'The presence of visceral evoked potentials elicited by cutaneous palpation of heartbeats in high and low awareness subjects', *Psychophysiology*, **25**, p. 459

JØRGENSEN, E. O. (1974): 'Technical contribution. Requirements for recording the EEG at high sensitivity in suspected brain death', *Electroencephalogr. Clin. Neurophysiol.*, **36**, pp. 65–69

KATKIN, E. S., CESTARO, V. L., and WEITKUNAT, R. (1991): 'Individual differences in cortical evoked potentials as a function of heartbeat detection ability', *Int. J. Neurosci.*, **61**, pp. 269–276

LEOPOLD, C. and SCHANDRY, R. (2001): 'The heartbeat-evoked brain potential in patients suffering from diabetic neuropathy and in healthy control persons', *Clin. Neurophysiol.*, **112**, pp. 674–682

MALMIVUO, J. and PLONSEY, R. (1995): 'Bioelectromagnetism. Principles and applications of bioelectric and biomagnetic fields' (Oxford University Press, New York, 1995)

MONTOYA, P., SCHANDRY, R., and MÜLLER, A. (1993): 'Heartbeat evoked potentials (HEP): topography and influence of cardiac awareness and focus of attention', *Electroencephalogr. Clin, Neurophysiol.*, **88**, pp. 163–172

NYBOER, J. (1970): 'Electrical impedance plethysmography' (Charles C Thomas, Springfield, 1970)

O'KELLY, S. W., SMITH, D. C., and PILKINGTON, S. N. (1995): 'The auditory evoked potential and paediatric anaesthesia', *Br. J. Anaesth.*, **75**, pp. 428–430

OOSTENDORP, T. F. and VAN OOSTEROM, A. (1996): 'The surface Laplacian of the potential: theory and application', *IEEE Trans. Biomed. Eng.*, **43**, pp. 394–405

PAN, J. and TOMPKINS, W. J. (1985): 'A real-time QRS detection algorithm', *IEEE Trans. Biomed. Eng.*, **32**, pp. 230–236

PEREZ, J. J., GUIJARRO, E., and BARCIA, J. A. (1999): 'Methodological aspects on heart action-related brain potentials extraction'. Proc. 5th Conf. Europ. Soc. Eng. Med., Barcelona, pp. 171–172

PEREZ, J. J., GUIJARRO, E., and BARCIA, J.A. (2000): 'Quantification of intracranial contribution to rheoencephalography by a numerical model of the head', *Clin. Neurophysiol.*, **111**, pp. 1306–1314

RAU, H., PAULI, P., BRODY, S., ELBERT, T., and BIRBAUMER, N. (1993): 'Baroreceptor stimulation alters cortical activity', *Psychophysiology*, **30**, pp. 322–325

REGAN, D. (1989): 'Human brain electrophysiology' (Elsevier, Amsterdam, 1989)

RIORDAN, H., SQUIRES, N. K., and BRENER, J. (1990): 'Cardio-cortical potentials: electrophysiological evidence for visceral perception', *Psychophysiology*, **27**, p. 59

RUSH, S. and DRISCOLL, D. A. (1968): 'Current distribution in the brain from surface electrodes', *Anesth. Anal. Curr. Res.*, **47**, pp. 717–723

SANDMAN, C. A., O'HALLORAN, J. P., and ISENHART, R. (1984): 'Is there an evoked vascular response?', *Science*, **224**, pp. 1355–1357

SANDMAN, C. A., VIGOR-ZIERK, C. S., ISENHART, R., WU, J., and ZETIN, M. (1992): 'Cardiovascular phase relationships to the cortical event-related potential of schizophrenic, depressed, and normal subjects', *Biol. Psychiatry*, **32**, pp. 778–789

SCHANDRY, R. and MONTOYA, P. (1996): 'Event-related brain potentials and the processing of cardiac activity', *Biol. Psychol.*, **42**, pp. 75–85

SCHANDRY, R., SPARRER, B. and WEITKUNAT, R. (1986): 'From the heart to the brain: a study of heartbeat contingent scalp potentials' *Int. J. Neurosci.*, **30**, pp. 261–275

SCHANDRY, R. and WEITKUNAT, R. (1990): 'Enhancement of heartbeat-related brain potentials through cardiac awareness training', *Int. J. Neurosci.*, **53**, pp. 243–253

WEITKUNAT, R. and SCHANDRY, R. (1990): 'Motivation and heartbeat evoked potentials', *J. Psychophysiol.*, **4**, pp. 33–40

Authors' biographies

JUAN J PÉREZ was born in Valencia, Spain, in 1967. He received the M.S. degree in electrical and electronic engineering in 1992 and the Ph.D. degree in biomedical engineering in 2003 from Polytechnic University of Valencia. He is currently an Associate Professor in the Department of Electronic Engineering of the same university. His

main research interests are signal processing applied to evoked potentials and electric field distribution in biological tissues.

ENRIQUE GUIJARRO received his Ph.D. degree in biomedical engineering from the Polytechnic University of Valencia in 1992, where currently he is an Associate Professor in the Department of Electronic Engineering. His research interests include biomedical instrumentation and diagnostic tools in the field of neuroengineering.

JUAN A BARCIA received his M.D. degree in 1986 and his Ph.D. degree in neurosurgery in 1996 from the University of Valencia, Spain. Currently, he is an Associate Professor in the Surgery Department of the same university. His main research interests are the technology application to neurosurgery; stereotaxy, radiosurgery, neuromonitorization and neuroendoscopy. He is director of the Neural Regeneration Unit of the Prince Felipe Research Centre of Valencia.